



**HAL**  
open science

## Pressure drop and axial dispersion in industrial millistructured heat exchange reactors

Maxime Moreau, Nathalie Di Miceli Raimondi, Nathalie Le Sauze, Michel Cabassud, Christophe Gourdon

► **To cite this version:**

Maxime Moreau, Nathalie Di Miceli Raimondi, Nathalie Le Sauze, Michel Cabassud, Christophe Gourdon. Pressure drop and axial dispersion in industrial millistructured heat exchange reactors. *Chemical Engineering and Processing: Process Intensification*, 2015, 95, pp.54-62. 10.1016/j.cep.2015.05.009 . hal-01338169

**HAL Id: hal-01338169**

**<https://hal.science/hal-01338169>**

Submitted on 28 Jun 2016

**HAL** is a multi-disciplinary open access archive for the deposit and dissemination of scientific research documents, whether they are published or not. The documents may come from teaching and research institutions in France or abroad, or from public or private research centers.

L'archive ouverte pluridisciplinaire **HAL**, est destinée au dépôt et à la diffusion de documents scientifiques de niveau recherche, publiés ou non, émanant des établissements d'enseignement et de recherche français ou étrangers, des laboratoires publics ou privés.



## Open Archive TOULOUSE Archive Ouverte (OATAO)

OATAO is an open access repository that collects the work of Toulouse researchers and makes it freely available over the web where possible.

This is an author-deposited version published in : <http://oatao.univ-toulouse.fr/>  
Eprints ID : 15850

**To link to this article** : DOI : 10.1016/j.cep.2015.05.009  
URL : <http://dx.doi.org/10.1016/j.cep.2015.05.009>

**To cite this version** : Moreau, Maxime and Di Miceli Raimondi, Nathalie and Le Sauze, Nathalie and Cabassud, Michel and Gourdon, Christophe *Pressure drop and axial dispersion in industrial millistructured heat exchange reactors*. (2015) *Chemical Engineering and Processing: Process Intensification*, vol. 95. pp. 54-62. ISSN 0255-2701

Any correspondence concerning this service should be sent to the repository administrator: [staff-oatao@listes-diff.inp-toulouse.fr](mailto:staff-oatao@listes-diff.inp-toulouse.fr)

# Pressure drop and axial dispersion in industrial millistructured heat exchange reactors

Maxime Moreau<sup>a,b</sup>, Nathalie Di Miceli Raimondi<sup>a,b,\*</sup>, Nathalie Le Sauze<sup>a,b</sup>,  
Michel Cabassud<sup>a,b</sup>, Christophe Gourdon<sup>a,b</sup>

<sup>a</sup> Université de Toulouse, INP, UPS, LGC (Laboratoire de Génie Chimique), 4 allée Emile Monso, F-31432 Toulouse, Cedex 04 France

<sup>b</sup> CNRS, LGC (Laboratoire de Génie Chimique), F-31432 Toulouse, Cedex 04 France

## A B S T R A C T

Hydrodynamic characterization by means of pressure drop and residence time distribution (RTD) experiments is performed in three millistructured heat exchange reactors: two Corning reactors (further referred to as Corning HP and Corning RT) and a Chart reactor. Pressure drop is measured for different flow rates and fluids. Fanning friction factor is then calculated and its evolution versus Reynolds number is plotted for each reactor, showing the influence of the geometrical characteristics of the reactors on this parameter. From RTD experiments, axial dispersion coefficients that allow calculating Péclet numbers are identified by solving the convection-dispersion equation. The results highlight plug flow behavior of these reactors for the range of flow rates studied. Péclet number in Corning HP remains constant in the range of Reynolds number studied. Its specific pattern is designed to generate mixing structures that allow homogenization of the tracer over the cross-section. It explains the plug flow behavior of this reactor even at low Reynolds number but generates high pressure drop. Péclet number in Corning RT and Chart ShimTec<sup>®</sup> increases with Reynolds number. This evolution is encountered for straight circular pipes in turbulent regime and confirms the pressure drop analysis.

### Keywords:

Heat exchange reactors  
Pressure drop  
Axial dispersion  
Modelling

## 1. Introduction

The need to develop safer, more effective and less energy consuming processes while respecting environmental requirements caused since a few years the interest of the industry for the intensified technologies. In this context, heat exchange reactors are promising technologies [1]. Indeed it is difficult to control temperature in batch or semi-batch reactors when reactions are highly exothermic. Heat exchange reactors may offer a better thermal control of the reactions increasing safety and selectivity while reducing by-products generation. Continuous millistructured heat exchange reactors provide heat transfer at the closest of the reaction. They combine the advantages of millireactors (fast mixing, reactive volume confinement) and compact heat exchangers (high transfer area and large material mass per unit of reactive volume).

However, the miniaturization of the devices leads to low Reynolds number for the process fluid. To avoid pure laminar flow, instabilities have to be generated for mixing and transfer issues. Therefore millistructured devices are generally characterized by a complex geometry of the process channels to promote mixing, providing specific hydrodynamic behaviors notably in terms of pressure drop and Residence Time Distribution (RTD). Pressure drop is a key parameter to design a process since the cost of the pumps driving the fluid through the installation is generally a great part of the whole capital cost. RTD gives precious information on the hydrodynamics of the reactor and particularly on the axial dispersion generated. Axial dispersion is responsible of the spreading of the reactants and the products along the device which can lead to selectivity and conversion issues. This hydrodynamic parameter must thus be determined to correctly model the reaction [2].

The aim of this study is to provide and analyze the hydrodynamic behavior of three industrial millistructured reactors: two Corning fluidic modules and a Chart reactor. Elgue et al. [3] demonstrated the performances of these devices for the implementation of a chemical reaction. The authors carried out a two-phase esterification and observed higher conversion with the intensified millireactors than in batch conditions. Braune et al. [4]

\* Corresponding author. Tel.: +33 562258920; fax.: +33 562258891.

E-mail addresses: [mmoreau3@ensiacet.fr](mailto:mmoreau3@ensiacet.fr) (M. Moreau),  
[nathalie.raimondi@iut-tlse3.fr](mailto:nathalie.raimondi@iut-tlse3.fr) (N. Di Miceli Raimondi),  
[nathalie.lesauze@iut-tlse3.fr](mailto:nathalie.lesauze@iut-tlse3.fr) (N. Le Sauze), [michel.cabassud@ensiacet.fr](mailto:michel.cabassud@ensiacet.fr)  
(M. Cabassud), [christophe.gourdon@ensiacet.fr](mailto:christophe.gourdon@ensiacet.fr) (C. Gourdon).

## Nomenclature

$c$	Concentration of tracer ( $\text{mol m}^{-3}$ )
$D_{ax}$	Axial dispersion coefficient ( $\text{m}^2 \text{s}^{-1}$ )
$D_h$	Hydraulic diameter of the tube (m)
$D_m$	Molecular diffusion coefficient of tracer in solvent ( $\text{m}^2 \text{s}^{-1}$ )
$E$	Distribution function ( $\text{s}^{-1}$ )
$f$	Fanning friction factor (-)
$J$	Number of stirred tanks (-)
$L$	Length of the reactor (m)
$P$	Perimeter of the cross section (m)
$Pe$	Péclet number (-)
$Q$	Flow rate ( $\text{m}^3 \text{s}^{-1}$ )
$Re_h$	Hydraulic Reynolds number (-)
$Re_{\sqrt{S}}$	Square section Reynolds number (-)
$S$	Cross section of the channel ( $\text{m}^2$ )
$s$	Minimization function ( $\text{mol}^2 \text{s m}^{-6}$ )
$t$	Time (s)
$t_{r,exp}$	Experimental residence time (s)
$u_0$	Average velocity ( $\text{m s}^{-1}$ )
$V$	Volume ( $\text{m}^3$ )
$x$	Longitudinal coordinate (m)

### Greek letters

$\mu$	Dynamic viscosity (Pa.s)
$\rho$	Density ( $\text{kg m}^{-3}$ )
$\Delta P$	Pressure drop (Pa)

### Subscripts

calc	Calculated
exp	Experimental
in	Inlet of the reactor
out	Outlet of the reactor
square	Square section

then Buisson et al. [5] also demonstrated the efficiency of mass transfer in Corning mixing module by performing selective reactions. Pressure drop and residence time distribution in Corning reactors have already been investigated [6,7] and residence time distribution have also been studied in Chart ShimTec<sup>®</sup> based technology by Cantu-Perez et al. [8]. However, the experiments were carried out with water for pressure drop measurements and generic correlations are missing to estimate the hydrodynamic behavior using quantitative parameters.

In the present work, pressure drop and RTD experiments are carried out. They are analyzed in order to suggest correlations for the estimation of dimensionless numbers characteristic of the hydrodynamics of reactors such as Fanning friction factor and Péclet number. The impact of the geometry of the three devices on the pressure drop and the RTD results is also discussed. The first

part of this paper presents the reactors design and the experimental setup. The pressure drop results are presented in a second part. Then, the RTD experiments and the methodology to identify the Péclet number are described. The results are compared to models available in literature.

## 2. Experimental method

### 2.1. Description of the reactors

The devices tested are two Corning fluidic modules G1 based on the Corning Advanced-Flow<sup>™</sup> technology [9] and a Chart reactor based on the ShimTec<sup>®</sup> technology [10] (Fig. 1).

Corning modules are made of three glass parts. The first Corning module (hereinafter called Corning RT for Residence Time) is composed of one plate carved by a single rectangular channel with 180° bends. The second module (hereinafter called Corning HP for Heart Pattern) is based on a Heart Pattern designed to generate mixing structures (51 hearts by plate). Each process plate is combined with two utility plates that allow to control the temperature of the reaction. These modules can be used in series to form a complete reactor. The Chart ShimTec<sup>®</sup> reactor is composed of thin plates (also called shims) that include the channels of the reactor. They are bonded together to create the whole structure. It is composed of three parallel process channels. The reactor can be fed by a utility fluid for heat exchange purpose. These three reactors are designed for specific applications. Corning RT is made to pre-heat reactants before a reaction plate or to add residence time at the end of the setup. Corning HP is likely used for two-phase reactions that need intensified mass transfer. Chart ShimTec<sup>®</sup> reactor is designed to produce low pressure drop to perform reactions with viscous fluids. Their characteristic dimensions are given in Table 1. It is difficult to estimate the length of Corning HP reactor since its section is not constant. However, the RTD results are used to identify the equivalent cross section and length of the reactor. Indeed, these parameters are fitted by comparing the shapes of the experimental and calculated outlet RTD curves and the experimental and theoretical residence times (see Appendix A). Nevertheless, even if these equivalent characteristics are not perfectly reliable, they do not affect the identification of hydrodynamic behaviors as function of the reactor geometry. For the Chart ShimTec<sup>®</sup> reactor, the equivalent length is the average length of the 3 channels. For the RTD experiments, it is considered that the output RTD curves can be decomposed into three distinct curves representing the path of the tracer in the three channels of

**Table 1**  
Reactors dimensions.

	Corning RT	Corning HP	Chart ShimTec <sup>®</sup>
Equivalent cross section $S$ ( $10^{-6} \text{m}^2$ )	3.8	4.6	$4.0 \times 3$ channels
Equivalent length $L$ (m)	2.0	2.5	1.5

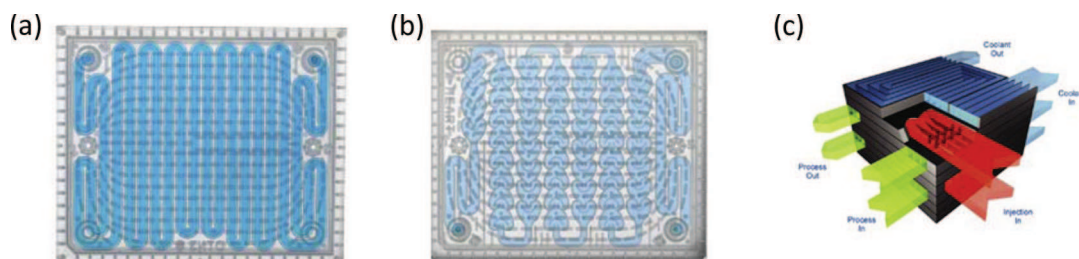


**Fig. 1.** Millistructured reactors: (a) Corning RT, (b) Corning HP and (c) Chart ShimTec<sup>®</sup> [9,10].

different length. However, it is assumed that the tracer concentration at the entrance of each channel is the same as the average velocity and the axial dispersion coefficient characterizing each channel.

## 2.2. Experimental setup

The experimental setup is illustrated on Fig. 2. It is composed of an external gear pump connected to a feeding tank. A by-pass system allows a better control of the flow rate. A T-shape injector is used to inject the tracer with a syringe right before the inlet of the reactor to carry out the RTD experiments. The outlet of the reactor is linked to a storage tank. A Coriolis-effect flow meter measures the mass flow rate and the density of the process fluid. A Rosemount differential pressure transducer connected to the inlet and the outlet of the reactor is used to measure the pressure drop generated. UV sensors measure the absorbance of the fluid at the inlet and the outlet of the reactor to follow the concentration of the tracer as a function of time.

## 2.3. Pressure drop measurement

The pressure drop is measured for different flow rates. Water ( $\mu = 1$  cP,  $\rho = 1000$  kg m<sup>-3</sup>) is used for the higher Reynolds numbers. Silicon oils ( $\mu = 9.3$  cP,  $\rho = 960$  kg m<sup>-3</sup>;  $\mu = 21$  cP,  $\rho = 970$  kg m<sup>-3</sup>) and a glycerol-water mixture with 75%wt glycerol ( $\mu = 40$  cP,  $\rho = 1200$  kg m<sup>-3</sup>) for the lower ones. Table 2 shows the range of flow rates and Reynolds numbers used for each reactor. Hydraulic diameter  $D_h$  is generally used as the characteristic length scale for non-circular channels. However Bahrami et al. [11] showed that it is more appropriate to use the square root of the cross section  $S$  for pressure drop considerations. Therefore, the characteristic length is equivalent to the width of a square channel. A new Reynolds number is defined and based on  $S$ , the average velocity  $u_0$ , the density  $\rho$  and the viscosity  $\mu$  of the fluid.

$$Re_{\sqrt{S}} = \frac{\rho u_0 \sqrt{S}}{\mu} \quad (1)$$

The average velocity is calculated from the experimental flow rate of the process fluid  $Q$  from Eq. (2).

$$u_0 = \frac{Q}{S} \quad (2)$$

$Re_{\sqrt{S}}$  can be related to the classical hydraulic Reynolds number  $Re_h$  using Eq. (3), where  $P$  is the channel perimeter.

**Table 2**

Experimental range of flow rates and Reynolds numbers for pressure drop measurement.

		Corning RT	Corning HP	Chart ShimTec®
Water	$Q$ (Lh <sup>-1</sup> )	0.5–15	1–15	2–78
	$Re_{\sqrt{S}}$	85–2 000	350–1 850	200–3 600
Silicon oils	$Q$ (Lh <sup>-1</sup> )	2–12	3–14	3–15
	$Re_{\sqrt{S}}$	25–170	40–180	4–130
Glycerol	$Q$ (Lh <sup>-1</sup> )	–	4–14.5	–
	$Re_{\sqrt{S}}$	–	15–63	–

$$Re_{\sqrt{S}} = \frac{P}{4\sqrt{S}} Re_h \quad (3)$$

With the hydraulic Reynolds number defined as a function of the hydraulic diameter  $D_h$  following Eq. (4).

$$Re_h = \frac{\rho u_0 D_h}{\mu} \quad (4)$$

The hydraulic diameter  $D_h$  is derived from:

$$D_h = \frac{4S}{P} \quad (5)$$

## 2.4. RTD experiments

Residence Time Distribution (RTD) is determined by the injection of a methylene blue tracer in the process fluid (water) at different flow rates. Its molecular diffusion coefficient in water is  $D_m = 3.10^{-10}$  m<sup>2</sup> s<sup>-1</sup> [12,13]. UV sensors measure the absorbance of the fluid passing through the reactor as a function of time. Both sensors are calibrated and the linear relationship between absorbance and the tracer concentration is established in order to calculate the average concentration at the measurement points.

The RTD response to a Dirac-like injection is given by the distribution function  $E(t)$  which is a normalized function of the concentration  $c(t)$ .

$$E(t) = \frac{c(t)}{\int_0^{\infty} c(t) dt} \quad (6)$$

Fig. 3 is an example of experimental injections. The continuous line corresponds to the reactor entrance. The curve's trail is due to the syringe-injection method. The dashed line corresponds to the outlet of the reactor. The spreading of the curve is due to the axial dispersion generated by the hydrodynamic conditions in the reactor. Table 3 shows the range of flow rate and Reynolds number studied for each reactor.

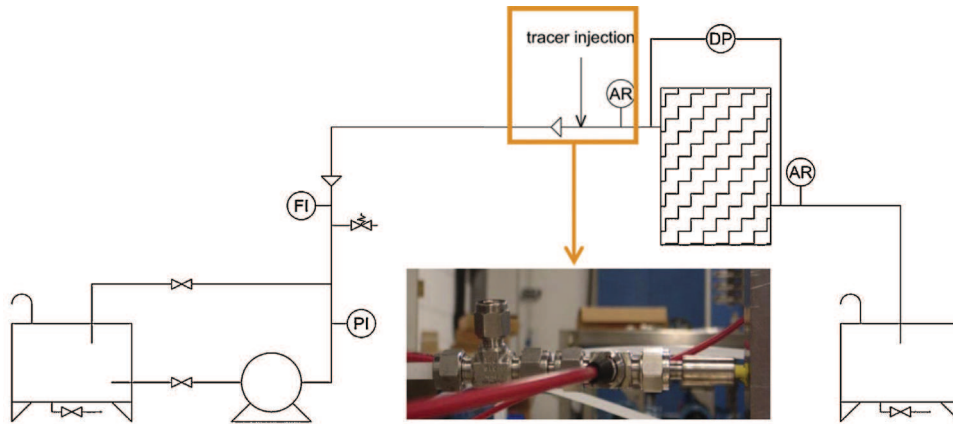


**Fig. 2.** Experimental setup.

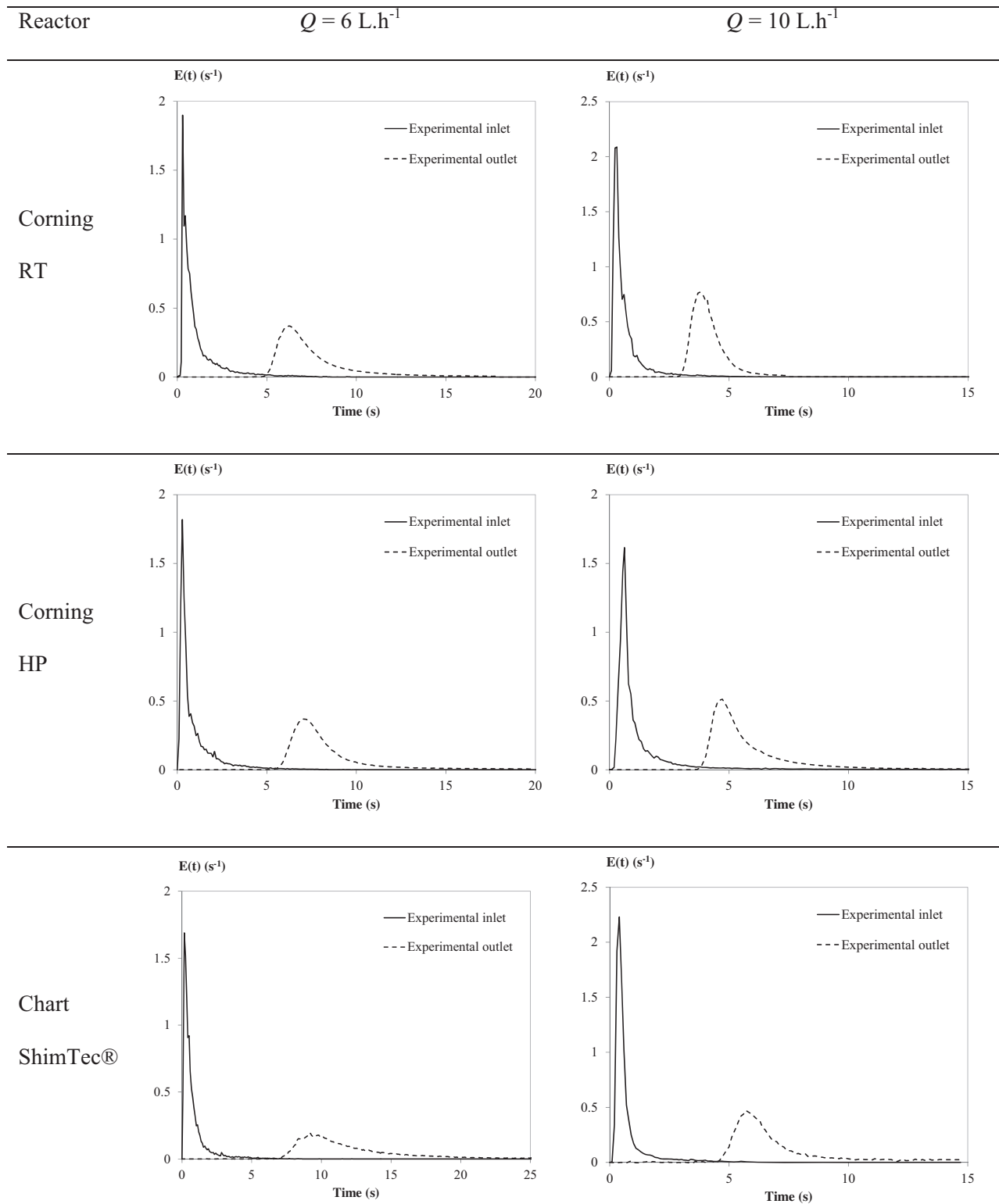


Fig. 3. Distribution functions  $E(t)$  obtained in the three reactors for  $Q=6 \text{ L.h}^{-1}$  and  $Q=10 \text{ L.h}^{-1}$ .

Table 3

Range of flow rates and Reynolds numbers for RTD experiments.

	Flow rate ( $\text{L.h}^{-1}$ )	$Re_{\sqrt{s}}$
Corning RT	6–12	850–1700
Corning HP	3–11	380–1420
Chart ShimTec®	4–13	180–600

### 3. Results and discussion

#### 3.1. Pressure drop

Fig. 4 shows the evolution of pressure drop versus flow rate for each reactor and each process fluid used. For a given fluid, Chart ShimTec® reactor generates less pressure drop than the other ones.

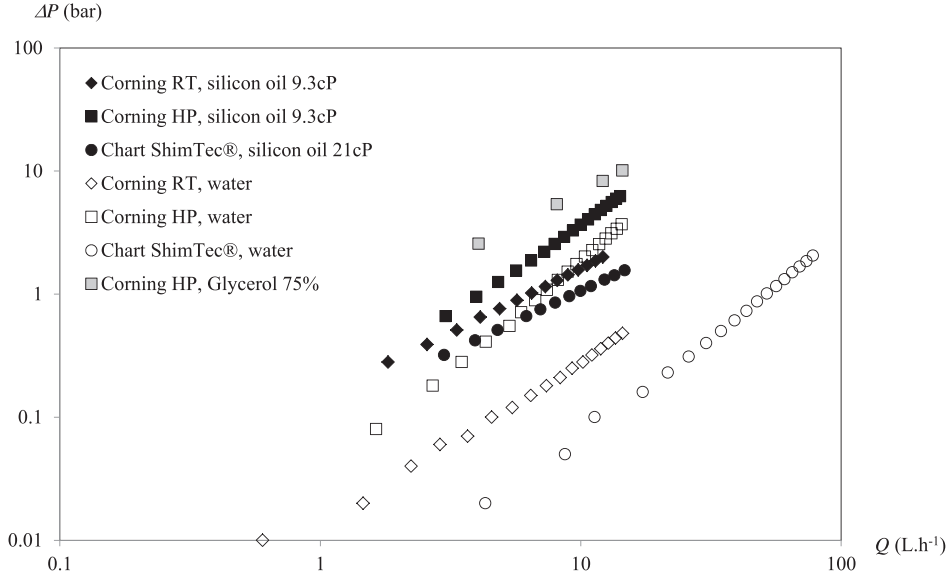


Fig. 4. Experimental pressure drop versus flow rate.

The division of the flow in three parallel channels allows to reduce the average velocity per channel compared to a single-channel configuration with the same hydraulic diameter while maintaining the same global flow rate. It confirms its capability to deal with viscous fluids or high flow rates. As expected, Corning HP reactor generates more pressure drop than the other reactors. Its pattern, designed to improve mixing and two-phase transfer performances leads to larger energy dissipation into the fluid producing significant pressure drop.

The pressure drop generated in a channel is function of Fanning friction factor  $f$ , density  $\rho$ , average velocity  $u_0$ , length of the reactor  $L$ , its cross section area  $S$  and its perimeter  $P$  following Eq. (7). Therefore, it is possible to determine  $f$  from a pressure drop measurement (Eq. (8)).

$$\Delta P = \frac{1}{2} f \rho u_0^2 \frac{L}{S} \quad (7)$$

$$f = \frac{2 \Delta P S}{\rho u_0^2 L} \quad (8)$$

Fanning friction factor depends on the geometry of the channel. For a straight square channel it has different empirical expressions have been established depending on the flow regime [14]. In laminar conditions ( $Re_{\sqrt{S}} < 2100$ ):

$$f_{\text{square}} = \frac{k_1}{Re_{\sqrt{S}}} \quad (9)$$

In transitional flow for smooth ducts ( $2100 < Re_{\sqrt{S}} < 10000$ ):

$$f_{\text{square}} = k_2 Re_{\sqrt{S}}^{-0.25} \quad (10)$$

(Blasius equation)

In fully turbulent flow ( $Re_{\sqrt{S}} > 10000$ ):

$$f_{\text{square}} = k_3 \quad (11)$$

$k_i$  are constant values depending on the shape of the channel cross section. Fig. 5 represents Fanning factor versus Reynolds number. From this figure, correlations are proposed to predict the pressure drop in the three reactors studied (Table 4).

The evolution of the Fanning friction factor for all the reactors can be compared to the one in a straight square channel. For low Reynolds number ( $Re_{\sqrt{S}} < 1000$  for Corning RT and Chart ShimTec®

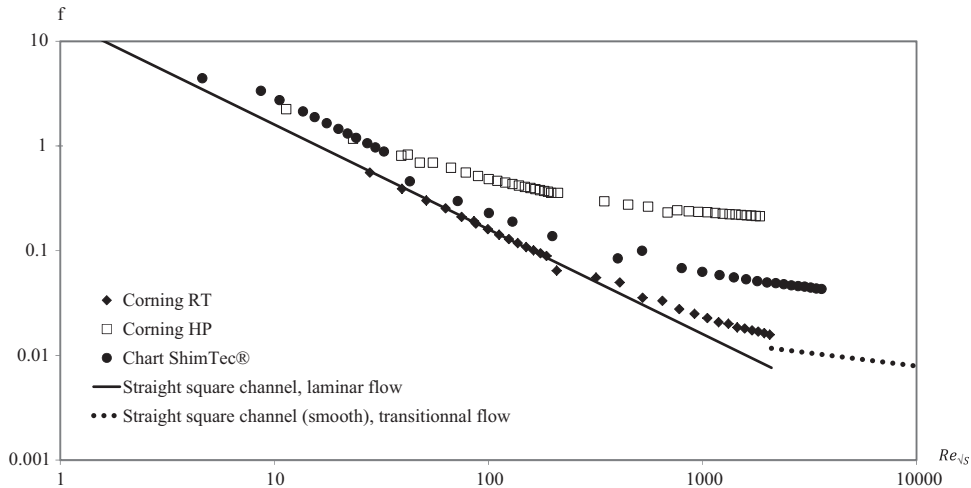


Fig. 5. Fanning friction factor versus Reynolds number.

**Table 4**  
Tendencies of Fanning friction factor depending on the flow regime.

Corning RT	Chart ShimTec®	Corning HP
$Re_{\sqrt{s}} < 1000 : f = \frac{16}{Re_{\sqrt{s}}}$	$Re_{\sqrt{s}} < 1000 : f = \frac{25}{Re_{\sqrt{s}}}$	$Re_{\sqrt{s}} < 50 : f = \frac{25}{Re_{\sqrt{s}}}$
$Re_{\sqrt{s}} > 1000 : f = \frac{0.08}{Re_{\sqrt{s}}^{0.25}}$	$Re_{\sqrt{s}} > 1000 : f = \frac{0.33}{Re_{\sqrt{s}}^{0.25}}$	$Re_{\sqrt{s}} > 1000 : f = 0.2$

reactor and  $Re_{\sqrt{s}} < 50$  for Corning HP) the trend observed corresponds to Eq. (9) associated to a laminar behavior.

An evolution to the transitional regime is observed at  $Re_{\sqrt{s}} = 1000$  respectively for Chart ShimTec® and Corning RT and at  $Re_{\sqrt{s}}$  around 50 for Corning HP. Above these values, Fanning factor values seem to follow the Blasius equation trend. The difference between Reynolds number values corresponding to the regime change for straight pipe and for the reactors studied must be due to the particular geometries of the reactors. Indeed, the Chart reactor

is composed of three channels with a few bends; Corning RT is composed of a rectangular channel with numerous 180° bends that generate energy dissipation at lower Reynolds than straight channels. The trend observed for Corning HP can be explained by the specific geometry of the channel which is designed to generate micro mixing structures even at low Reynolds number. The laminar regime is only observed for Reynolds number lower than 50. Fanning factor seems to reach a constant value, characteristic of a turbulent regime for Reynolds higher than 1000 instead of 10 000 in a straight pipe.

### 3.2. RTD experiments

The global hydrodynamic behavior of chemical reactors is often characterized by the RTD. It corresponds to the time necessary for different elements of fluid to pass through the reactor. It determines if the reactor behavior is close to a perfect stirred tank or to a plug flow reactor. RTD provides information about the

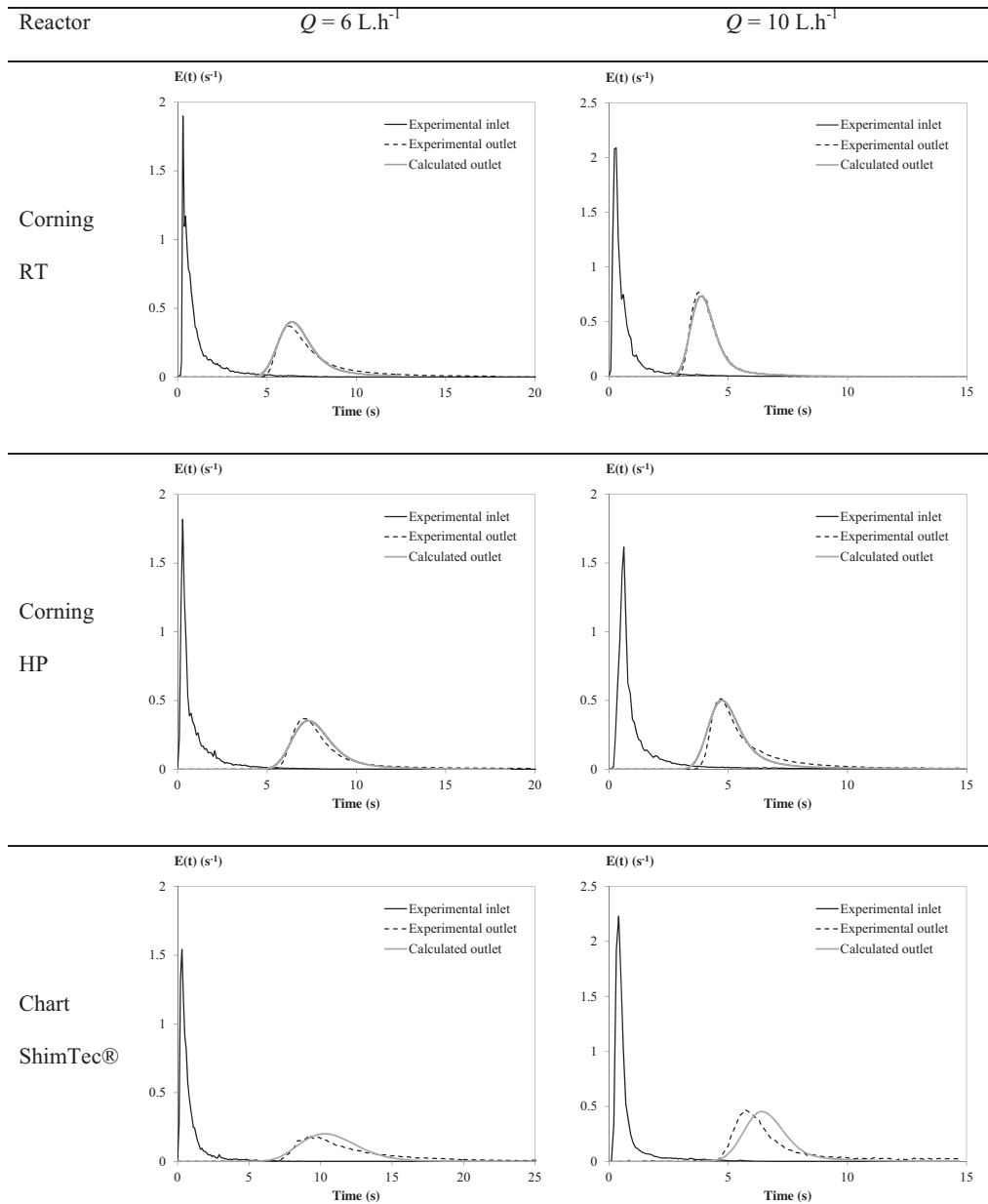


**Fig. 6.** Calculated outlet signal after  $D_{ax}$  identification obtained in the three reactors for  $Q = 6 \text{ L.h}^{-1}$  and  $Q = 10 \text{ L.h}^{-1}$ .

mixing efficiency and defects such as stagnant regions or shortcuts that can lower the performances of the reactor. RTD characterization is then necessary to model appropriately reactive systems.

In a plug flow reactor, each element of fluid has the same residence time. RTD experiments in a tubular reactor allow to highlight a deviation from this ideal behavior. The deviation is generally quantified by the Péclet number  $Pe$ . It compares the convective transport and the diffusive transport over the length of a device and is defined as follows:

$$Pe = \frac{u_0 L}{D_{ax}} \quad (12)$$

$Pe$  is directly related to the axial dispersion coefficient that takes into account all the phenomena inducing dispersion in a reactor. Axial dispersion is due to molecular diffusion, turbulence and non-uniformity of the velocity profile. It is thus a key factor when reactions with selectivity issues are considered [15,16]. This dimensionless number quantifies the difference between a perfect stirred reactor and a plug flow reactor. The plug flow behavior is assumed when  $Pe > 100$  [15].

Current methodologies for the characterization of axial dispersion are based on the identification of the axial dispersion coefficient from RTD experiments. It consists in comparing the outlet signal with an analytical solution provided by a convection–dispersion model [8,17,18] or a succession of perfectly mixed tanks model [19]. These models imply a perfect Dirac injection that is experimentally difficult to perform. To take into account the real injection, a deconvolution method is often used to treat the entrance signal [8,17]. But this mathematical treatment can lead to a loss of information, especially a loss concerning the trail of the injection.

Another method is proposed in this work to treat the RTD experiments without deconvolution step. It consists in solving the one dimension convection–dispersion equation (Eq. (13)) using the commercial software Comsol Multiphysics.

$$\frac{\partial c}{\partial t} + u_0 \frac{\partial c}{\partial x} - D_{ax} \frac{\partial^2 c}{\partial x^2} = 0 \quad (13)$$

With Initial condition:

$$t = 0 : c(x) = 0 \quad (14)$$

And Boundary conditions:

$$x = 0 : c(t) = c_{in,exp}(t) \quad (15)$$

$$x = L : \frac{\partial c}{\partial x} = 0 \quad (16)$$

$c$  is the average concentration of tracer over the cross section.  $t$  is time and  $x$  the longitudinal coordinate along the reactor ( $0 \leq x \leq L$ ). At  $t=0$ , no tracer is present in the reactor (Eq. (14)). The inlet concentration is set equal to the experimental concentration  $c_{in,exp}(t)$  (Eq. (15)). At the outlet of the reactor the gradient of concentration is supposed to be zero (Eq. (16)).

Firstly, an initial value of  $D_{ax}$  is chosen and the calculated concentration at  $x=L$ ,  $c_{out,calc}(t)$ , is compared to the experimental concentration  $c_{out,exp}(t)$ . The value of  $D_{ax}$  is then adjusted following the least squares method in order to minimize the  $s$  function defined as follows:

$$S = \int_0^\infty (c_{out,calc}(t) - c_{out,exp}(t))^2 \times dt \quad (17)$$

Fig. 6 gives examples of calculated  $E(t)$  curve with identified  $D_{ax}$  by minimization of the  $s$  function. This method is applied to characterize the three reactors.  $D_{ax}$  is represented as a function

of flow rate on Fig. 7. The axial dispersion coefficient remains constant for both Corning RT and Chart ShimTec® reactors while the flow rate increases. For the Corning HP, this coefficient increases with the flow rate. Table 5 summarizes these tendencies and proposes a correlation to calculate  $D_{ax}$  in the studied range of flow rate for the Corning HP.

Fig. 8 shows the results of Péclet numbers as function of Reynolds number for each industrial reactor. Each of these three devices can be considered as a plug flow reactor for  $Re_{\sqrt{5}} > 400$  since all the values of Péclet are rather close to 100. In Figs. 7 and 8, the irregularity of the curves is due to the uncertainty on the experimental axial dispersion coefficients. It is related to the noise on the absorbance signals which generates an uncertainty of about  $\pm 0.05 \text{ s}^{-1}$  on  $E(t)$  functions. Extreme values of  $D_{ax}$  are identified by adding and subtracting this uncertainty on RTD curves. The resulting uncertainty on  $D_{ax}$  is around  $\pm 20\%$ .

In Corning RT and Chart ShimTec® reactors, Péclet number increases with Reynolds number. The plug flow behavior of these reactors results of the velocity of the fluid. Péclet number of the Corning HP reactor is quite constant around the value 100 in the studied range of Reynolds number. This can be explained observing the geometry of the channel. The Heart Pattern had been designed to generate mixing structures at low velocity. These mixing structures imply the homogenization of the tracer's concentration across the section of the channel. In fact, each heart can be considered as individual perfect mixed volume. The whole reactor is so composed of a succession of 51 equivalent stirred tanks. It results in a theoretical Péclet number of 100 using Eq. (18) where  $J$  corresponds to the number of stirred tanks in series [20].

$$Pe = 2(J - 1) \quad (18)$$

Therefore, the plug flow of this reactor is due to the geometry of its channel, instead of being due to the velocity of the incoming process fluid as it is for the two other reactors.

### 3.4. Discussion

The axial dispersion coefficients obtained from the experiments are compared to models available in literature for circular pipes: (i) the model suggested by Taylor [21] for laminar flow and (ii) the model proposed by Levenspiel [15] for turbulent flow.

For laminar flow in tubular pipes ( $Re < 2100$ ), Taylor model gives a relationship between the axial dispersion coefficient  $D_{ax}$ , the molecular diffusion coefficient  $D_m$ , the hydraulic diameter and the average velocity [21].

$$D_{ax} = D_m + \frac{u_0^2 D_h^2}{192 D_m} \quad (19)$$

Eq. (19) was demonstrated by Taylor [21] in the case of steady flow. This equation gives very accurate approximation considering

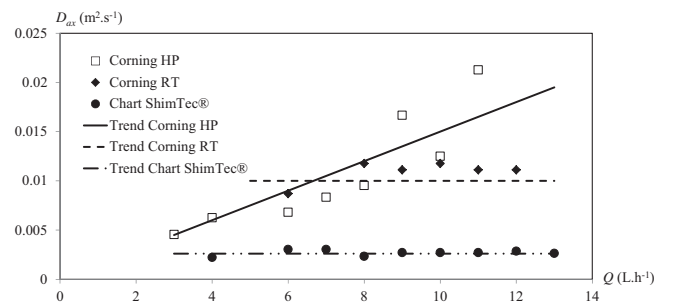
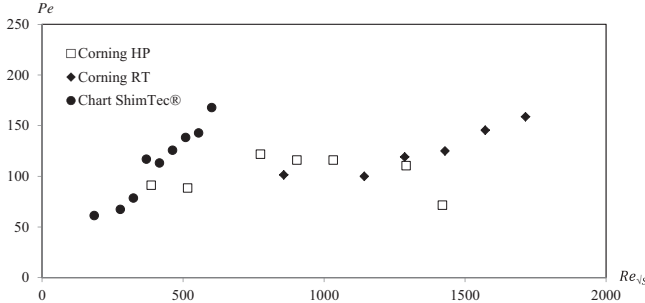


Fig. 7. Evolution of axial dispersion coefficient as a function of flow rate.

**Table 5**Correlation of  $D_{ax}$  [ $\text{m}^2 \text{s}^{-1}$ ]. For Corning HP,  $D_{ax}$  is expressed as a function of  $Q$  [ $\text{L h}^{-1}$ ].

	Corning RT	Chart ShimTec®	Corning HP
$D_{ax}$ [ $\text{m}^2 \text{s}^{-1}$ ]	$0.0100 \pm 0.0020$	$0.0026 \pm 0.0005$	$(0.0015 \pm 0.0005)Q$

**Fig. 8.** Evolution of Péclet number as function of Reynolds number.

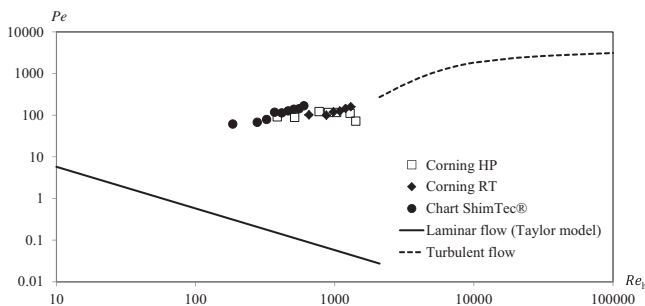
that  $D_{ax}$  only depends on geometrical and physical parameters [22,23].

In turbulent regime ( $Re_h > 2100$ ) and for straight circular pipes the relationship between the axial dispersion coefficient and Reynolds number is written as follows [15,24]:

$$\frac{D_{ax}}{u_0 D_h} = \frac{3 \cdot 10^7}{Re_h^{2.1}} + \frac{1.35}{Re_h^{0.125}} \quad (20)$$

Fig. 9 shows the evolution of Péclet number as a function of Reynolds number for a straight circular pipe using both models (Eqs. (19) and (20)). The length of the reactor is set at  $L = 2$  m and  $D_h = 2$  mm which roughly corresponds to the dimensions of the Corning and Chart reactors studied. The experimental data are added to the graph. The models predict that Péclet number decreases when Reynolds number increases in laminar flow. At higher Reynolds number, Péclet number first increases with Reynolds number ( $2100 < Re_h < 10\,000$ ) and then tends to reach a constant value.

The evolution of Péclet versus Reynolds obtained for Corning RT and Chart ShimTec® reactors in the range of Reynolds number explored is similar to the evolution obtained in a straight pipe in the transitional regime. It is consistent with the interpretation of the pressure drop results (Section 3.1). The constant value of  $Pe$  experimentally obtained for the Corning HP reactor corresponds to the tendency observed in turbulent regime at high Reynolds numbers in a straight pipe. This is still in agreement with the pressure drop characterization described in Section 3.1.

**Fig. 9.** Péclet number as function of Reynolds number: models ( $L = 2$  m,  $D_h = 2$  mm,  $D_m = 3 \cdot 10^{-10} \text{ m}^2 \text{ s}^{-1}$ ,  $\rho = 1000 \text{ kg m}^{-3}$ ,  $\mu = 10^{-3} \text{ Pa s}$ ) and experimental results.

## 4. Conclusion

This work describes and compares the hydrodynamics of three millistructured reactors. Pressure drop is measured in order to estimate the Fanning friction factor. RTD experiments are carried out in order to study the flow behavior of these three devices. The methodology used in this work to identify the axial dispersion coefficient from the RTD curves is based on the computation of the convection–dispersion equation. It allows to take into account the real signal shape of the tracer injection to avoid any treatment of the experimental data such as deconvolution that could lead to a loss of information.

The three reactors have different geometries in accordance to the application they are designed for. Corning HP reactor can be considered as a mixer-exchanger. Corning RT is likely used to pre-heat reactant before a reaction or to add residence time after the reaction occurred. Chart ShimTec® is used to perform reaction with viscous fluids. These characteristics have an obvious impact on the hydrodynamics of the reactors. Plug flow behavior of these three reactors is highlighted by the RTD analysis. The Heart Pattern particular geometry generates mixing structures that induces a plug flow behavior independently of the flow rate but is also responsible for the high pressure drop observed in this module. Pressure drop measurements show that the transition to turbulent regime is observed for  $Re_{\sqrt{S}} = 50$ . In Corning RT and Chart ShimTec®, the RTD experiments show that Péclet number increases with Reynolds number. The velocity of the fluid enhances plug flow behavior for these reactors. This last result is in accordance with literature data for straight circular pipes in turbulent regime and corroborates pressure drop results where the transition to turbulent regime occurs around  $Re_{\sqrt{S}} = 1000$ .

In order to complete the hydraulic characterization of these reactors, further study will be performed in terms of mixing time as function of flow rate and fluid properties.

## Acknowledgements

This work has been supported by the ANR (Agence Nationale de la Recherche), France: Project ANR PROCIP, ANR-2010-CD21-013-01. The experimental facility was supported by: the FNADT, Grand Toulouse, Prefecture Midi-Pyrenees and FEDER fundings.

## Appendix A.

Corning HP reactor: estimation of the equivalent cross section and length

Equivalent length and cross section for Corning HP reactor are identified by using the RTD results (8 experiments). Indeed, these parameters are fitted by comparing the experimental and theoretical residence times (Eq. (A.1)) and the shapes of the experimental and calculated outlet curves  $E(t)$  where the average velocity  $u_0$  in the one dimension convection-dispersion equation given by Eq. (13) is obtained from the cross section (Eq. (A.2)).

$$t_{r,\text{exp}} = \frac{LS}{Q} \quad (A.1)$$

$$u_0 = \frac{Q}{S} \quad (A.2)$$

The results in terms of cross section and length are given in Table 1.

## References

- [1] Z. Anxionnaz, M. Cabassud, C. Gourdon, P. Tochon, Heat exchanger/reactors (HEX reactors): concepts technologies: state-of-the-art, Chem. Eng. Process. Process Intensif. 47 (2008) 2029–2050.

- [2] K.D. Nagy, B. Shen, T.F. Jamison, K.F. Jensen, Mixing and dispersion in small-scale flow systems, *Org. Process Res. Dev.* 16 (2012) 976–981.
- [3] S. Elgue, A. Conte, A. Marty, J.S. Condoret, Two-phase enzymatic reaction using process intensification technologies, *Chem. Today* 31 (2013) 6.
- [4] S. Braune, P. Pöchlauer, R. Reintjens, S. Steinhofner, M. Winter, O. Lobet, et al., Selective nitration in a microreactor for pharmaceutical production under cGMP conditions, *Chem. Today* 27 (2009) 26–29.
- [5] B. Buisson, S. Donegan, D. Wray, A. Parracho, J. Gamble, P. Caze, et al., Slurry hydrogenation in a continuous flow reactor for pharmaceutical application, *Chem. Today* 27 (2009) 12–14.
- [6] M.S. Chivilikhin, L. Kuandykovi, E.D. Lavric, R. Federation, F. Avon, Residence time distribution in Corning<sup>®</sup> advanced-flow<sup>™</sup> reactors. Experiment and modelling, *Chem. Eng. Trans.* 25 (2011) 791–796.
- [7] E.D. Lavric, P. Woehl, Advanced-flow<sup>™</sup> glass reactors for seamless scaleup, *Chem. Today* 27 (2009) 45–48.
- [8] A. Cantu-Perez, S. Bi, S. Barrass, M. Wood, A. Gavriilidis, Residence time distribution studies in microstructured plate reactors, *Appl. Therm. Eng.* 31 (2011) 634–639.
- [9] Corning, Corning<sup>®</sup> Advanced-Flow<sup>™</sup> G1 Reactor, <http://www.corning.com/WorkArea/showcontent.aspx?id=48113> (2012).
- [10] Chart, Compact Heat Exchange Reactors, <http://www.chart-ec.com/pdf/Compact-Heat-Exchange-Reactors.pdf>, (2009).
- [11] M. Bahrami, M.M. Yovanovich, J.R. Culham, Pressure drop of fully-developed laminar flow in microchannels of arbitrary cross-section, *J. Fluids Eng.* 128 (2006) 1036.
- [12] G. Fate, D.G. Lynn, Molecular diffusion coefficients: experimental determination and demonstration, *J. Chem. Educ.* 67 (1990) 536.
- [13] V. Balakotaiah, H.C. Chang, Dispersion of chemical solutes in chromatographs and reactors, *Philos. Trans. A* 351 (1995) 39–75.
- [14] R.B. Bird, W.E. Stewart, E.N. Lightfoot, *Transport Phenomena*, 2nd ed., John Wiley & Sons Inc., New York, 2007.
- [15] O. Levenspiel, *Chemical Reaction Engineering*, 3rd ed., John Wiley & Sons Inc., New York, 1999.
- [16] D.W. Rippin, Simulation of single- and multiproduct batch chemical plants for optimal design and operation, *Comput. Chem. Eng.* 7 (1983) 137–156.
- [17] C.H. Hornung, M.R. Mackley, The measurement and characterisation of residence time distributions for laminar liquid flow in plastic microcapillary arrays, *Chem. Eng. Sci.* 64 (2009) 3889–3902.
- [18] W. Roetzel, F. Balzereit, Determination of axial dispersion coefficients in plate heat exchangers using residence time measurements, *Rev. Générale Therm.* 36 (1997) 635–644.
- [19] Z. Anxionnaz-Minvielle, M. Cabassud, C. Gourdon, P. Tochon, Influence of the meandering channel geometry on the thermo-hydraulic performances of an intensified heat exchanger/reactor, *Chem. Eng. Process. Process Intensif.* 73 (2013) 67–80.
- [20] J. Villiermaux, *Génie de la Réaction Chimique*, 2nd ed., Tec&Doc, Paris, 1993.
- [21] G. Taylor, Dispersion of soluble matter in solvent flowing slowly through a tube, *Proc. A* 219 (1953) 186–203.
- [22] W.N. Gill, R. Sankarasubramanian, Exact analysis of unsteady convective diffusion, *Proc. Roy. Soc. London A* 316 (1970) 341–350.
- [23] W.N. Gill, Unsteady tubular reactors—time variable flow and inlet conditions, *Chem. Eng. Sci.* 30 (9) (1975) 1123–1128.
- [24] P. Trambouze, *Les Réacteurs Chimiques – De la Conception à la Mise en œuvre*, Technip, Paris, 1984.